Report

Cell Reports

Targeting One Carbon Metabolism with an Antimetabolite Disrupts Pyrimidine Homeostasis and Induces Nucleotide Overflow

Graphical Abstract

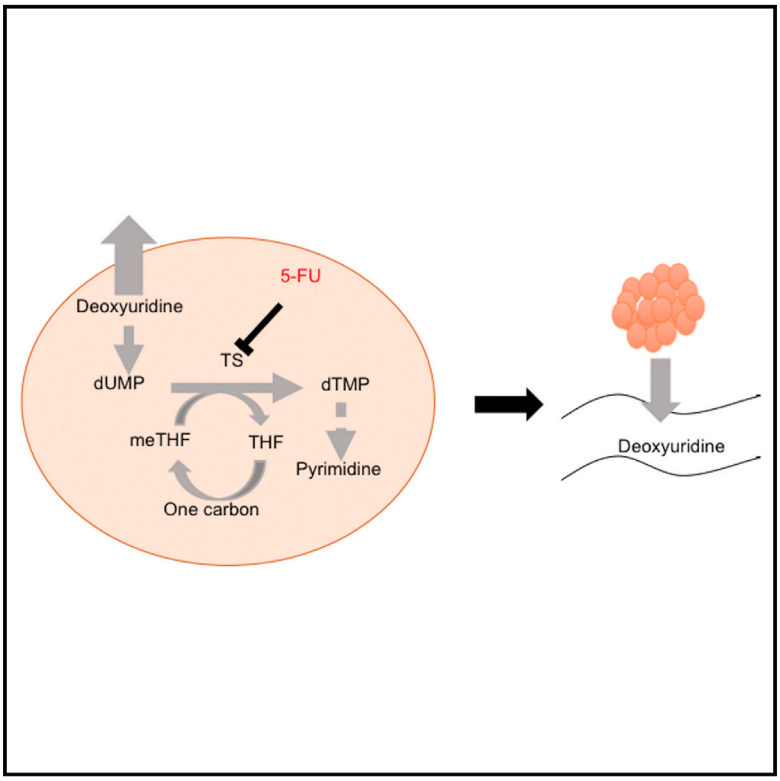

Authors

Zheng Ser, Xia Gao, Christelle Johnson, Mahya Mehrmohamadi, Xiaojing Liu, Siqi Li, Jason W. Locasale

Correspondence

jason.locasale@duke.edu

In Brief

Ser et al. show that 5-fluorouracil, a commonly used antimetabolite in chemotherapy, disrupts thymidylate synthase activity, causing nucleotide imbalance and the induction of overflow metabolism in cells and in the serum of mice bearing colorectal tumors.

Highlights

- One carbon metabolism fluxes correlate with 5-fluorouracil (5-FU) sensitivity
- 5-FU causes nucleotide imbalance by inhibiting thymidylate synthase
- 5-FU induces overflow metabolism in pyrimidine synthesis
- Alterations in overflow metabolism from colorectal tumors can be measured in serum

Ser et al., 2016, Cell Reports *15*, 2367–2376
June 14, 2016
http://dx.doi.org/10.1016/j.celrep.2016.05.035

CellPress

Cell Reports
Report

Targeting One Carbon Metabolism with an Antimetabolite Disrupts Pyrimidine Homeostasis and Induces Nucleotide Overflow

Zheng Ser,[1,5] Xia Gao,[2,5] Christelle Johnson,[3] Mahya Mehrmohamadi,[2,4] Xiaojing Liu,[2] Siqi Li,[2] and Jason W. Locasale[2,*]
[1]Tri-Institutional Training Program in Chemical Biology, Weill Cornell Medical College, Rockefeller University, Memorial Sloan-Kettering Cancer Center, New York, NY 10065, USA
[2]Department of Pharmacology and Cancer Biology, Duke Cancer Institute, Duke Molecular Physiology Institute, Duke University School of Medicine, Durham, NC 27710, USA
[3]Department of Biomedical Engineering, Cornell University, Ithaca, NY 14853, USA
[4]Graduate Field of Genetics Genomics and Development, Department of Molecular Biology and Genetics, Cornell University, Ithaca, NY 14853, USA
[5]Co-first author
*Correspondence: jason.locasale@duke.edu
http://dx.doi.org/10.1016/j.celrep.2016.05.035

SUMMARY

Antimetabolites that affect nucleotide metabolism are frontline chemotherapy agents in several cancers and often successfully target one carbon metabolism. However, the precise mechanisms and resulting determinants of their therapeutic value are unknown. We show that 5-fluorouracil (5-FU), a commonly used antimetabolite therapeutic with varying efficacy, induces specific alterations to nucleotide metabolism by disrupting pyrimidine homeostasis. An integrative metabolomics analysis of the cellular response to 5-FU reveals intracellular uracil accumulation, whereas deoxyuridine levels exhibited increased flux into the extracellular space, resulting in an induction of overflow metabolism. Subsequent analysis from mice bearing colorectal tumors treated with 5-FU show specific secretion of metabolites in tumor-bearing mice into serum that results from alterations in nucleotide flux and reduction in overflow metabolism. Together, these findings identify a determinant of an antimetabolite response that may be exploited to more precisely define the tumors that could respond to targeting cancer metabolism.

INTRODUCTION

Antimetabolite chemotherapy is one of the most-successful therapeutic strategies for the treatment of neoplastic disease (Kaye, 1998). It is also highly toxic while exhibiting variable efficacy. Thus, identifying the precise situations where it might be effective as a medicine is a pressing biomedical need. One commonly prescribed example is 5-fluorouracil (5-FU), which remains a frontline chemotherapy for multiple advanced stage cancers, notably colorectal cancer (CRC) (Longley et al., 2003). However, there lacks a comprehensive and mechanistic understanding of its effects on metabolism that could have prognostic value clinically (Locasale, 2013). This agent and other antimetabolite compounds are thought to target metabolic enzymes that are either involved in nucleotide metabolism or the folate cycle—directly affecting nucleotide biosynthesis and indirectly affecting other metabolic processes that are coupled to the flux into the nucleotide pool and one carbon metabolism. Therefore, we reasoned its direct effects on metabolism might encode information that could lead to biomarker identification for cytotoxic response that would improve the precision of its indication. If successful, this endeavor would bring precision medicine to a set of agents that have historically been thought to lack specificity.

Many of the current chemotherapies target a metabolic network known as one carbon metabolism. The serine, glycine, and one carbon (SGOC) metabolic network involving the folate and methionine cycles integrates nutritional status from amino acids, glucose, and vitamins and generates diverse outputs, such as the biosynthesis of lipids, nucleotides, and proteins; the maintenance of redox status; and the substrates for methylation reactions. Recently, multiple studies have found newfound roles of genes in this pathway in tumorigenesis (Locasale, 2013; Mehrmohamadi et al., 2014). Examples include the presence of cancer-driving genes, such as *PHGDH*, whose product diverts glucose metabolism into one carbon metabolism (Locasale et al., 2011; Possemato et al., 2011). Furthermore, in an analysis of uptake and excretion rates measured across population of cancer cells, glycine uptake was found to most strongly correlate with cell proliferation (Jain et al., 2012). Serine has also been found to be essential for cell proliferation (Labuschagne et al., 2014; Maddocks et al., 2013, 2016), and *SHMT2*, which encodes a mitochondrial serine hydroxymethyltransferase, was shown to provide context-dependent susceptible liabilities for tumor maintenance (Kim et al., 2015; Ye et al., 2014). Together, these newfound roles for genes in this network in cancer provide further rationale for targeting the pathway in cancer in a specific manner.

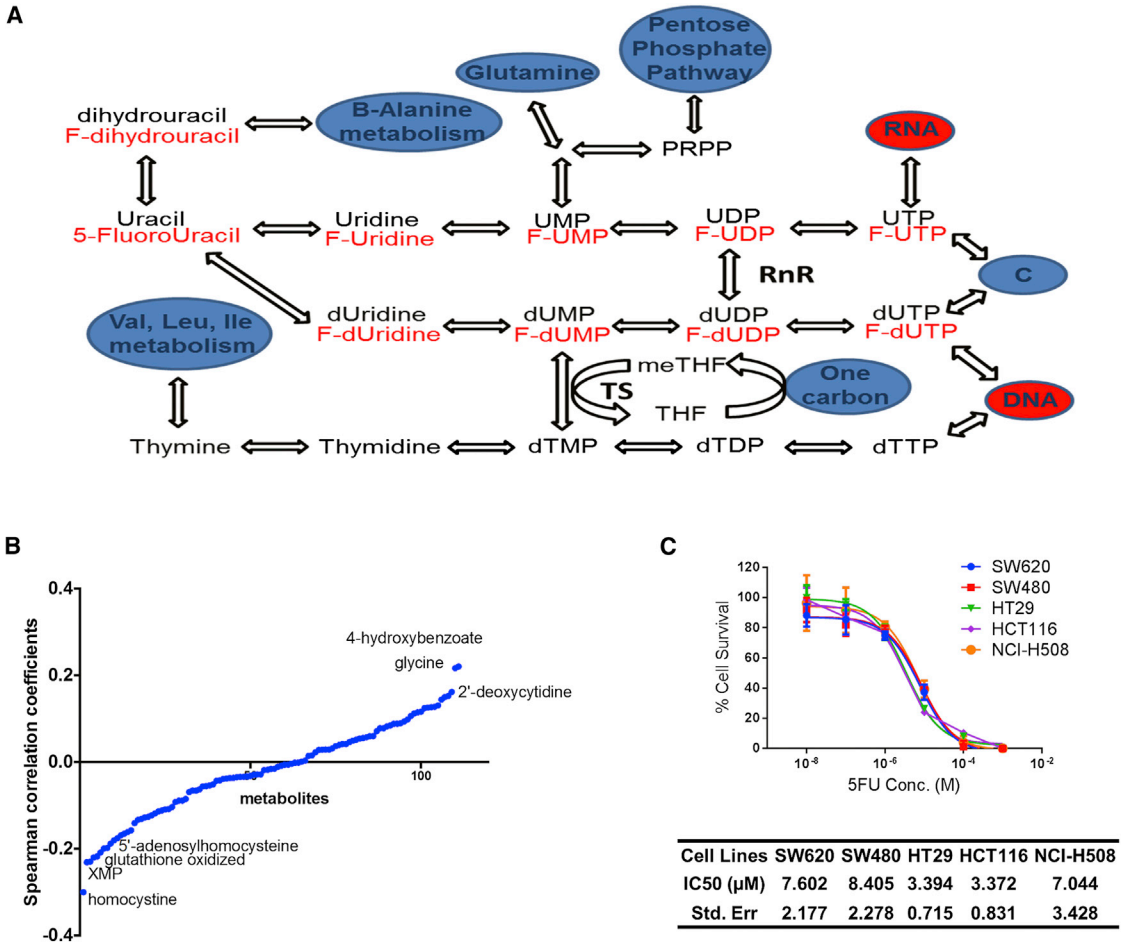

Cell Lines	SW620	SW480	HT29	HCT116	NCI-H508
IC50 (μM)	7.602	8.405	3.394	3.372	7.044
Std. Err	2.177	2.278	0.715	0.831	3.428

Figure 1. Incorporation of 5-Fluorouracil into the Pyrimidine Pathway

(A) Metabolic pathway map of pyrimidine pathway, focusing on uracil, 5-FU, and their derivatives, with C representing cytidine and its derivatives. Metabolites are dihydrouracil, fluoro-dihydrouracil (F-dihydrouracil), uracil, 5-FU, uridine-monophosphate (UMP), fluoro-uridine-monophosphate (F-UMP), uridine-diphosphate (UDP), fluoro-uridine-diphosphate (F-UDP), uridine-triphosphate (UTP), fluoro-uridine-triphosphate (F-UTP), deoxyuridine (dUridine), fluoro-deoxyuridine (F-dUridine), deoxyuridine-monophosphate (dUMP), fluoro-deoxyuridine-monophosphate (F-dUMP), deoxyuridine-diphosphate (dUDP), fluoro-deoxyuridine-diphosphate (F-dUDP), deoxyuridine-triphosphate (dUTP), fluoro-deoxyuridine-triphosphate (F-dUTP), thymine, thymidine, deoxy-thymidine-monophosphate (dTMP), deoxy-thymine-diphosphate (dTDP), deoxy-thymine-triphosphate (dTTP), phosphoribosyl pyrophosphate (PRPP), methylene-tetrahydrofolate (meTHF), and tetrahydrofolate (THF).

(B) Correlations of uptake and excretion rates of metabolites with IC_{50} of 5-FU response across NCI-60 cell line panel.

(C) IC_{50} data for five cell lines. Error bars represent ± SEM.

In this study, we investigated how a commonly used cancer chemotherapeutic 5-FU affects one carbon metabolism and a key component of its function, nucleotide synthesis. We questioned whether there is any specific molecular mechanism that defines its actions. Using a recently developed high-resolution liquid-chromatography-mass-spectrometry-based technology (Liu et al., 2014; Ser et al., 2015), simultaneous targeted profiling of hundreds of metabolites is possible (Liu et al., 2014). This approach is able to robustly quantify metabolites in concentration ranges over four orders of magnitude and has been previously applied to study the SGOC network (Mentch et al., 2015). Metabolite profiling and flux profiling have offered valuable insights into metabolism and its role in pathophysiology (Johnson et al., 2016; Zamboni et al., 2015). We therefore hypothesized that exploiting the use of this technology could identify unexplored mechanisms that mediate the action of 5-FU and thus bring additional context to precisely define its indication.

RESULTS

Disruption of Pyrimidine Metabolism Defines the Commonality of Response to 5-FU among Different Cancer Cells

5-FU is an antimetabolite agent that targets nucleotide metabolism and is metabolized as a mimetic of uracil (Figure 1A). To first assess the molecular features that might determine its efficacy, we examined the NCI-60 cell line compendium and correlated the extent of cytotoxicity on each cell line as

measured by the inhibitory curve at 50% (IC_{50}) value with the uptake and excretion rates of a set of metabolites (Figure 1B). The Spearman correlation analysis indicated that the IC_{50} value was most positively correlated with 4-hydroxybenzoate, glycine, and 2′-deoxycytidine but negatively correlated with homocysteine, xanthosine monophosphate (XMP), oxidized glutathione, and 5′-adenosyl homocysteine. These findings indicate that fluxes related to SGOC metabolism associate with the response to 5-FU. They also suggest that 5-FU likely has effects on multiple aspects of the SGOC network, including effects on metabolite flow in one-carbon metabolism (glycine, homocysteine, and 5′-adenosyl homocysteine), nucleotide metabolism (2′-deoxycytidine and XMP), and in cellular redox (glutathione). Although the correlation coefficient is small for each individual metabolite, the overall trend in the rankings of the correlation indicates that the SGOC network is related to 5-FU sensitivity, suggesting that some predictive ability may be present in the secretory fluxes of the SGOC network.

We extended these initial findings by carrying out a metabolomics analysis of 5-FU on a panel of CRC cells. CRC cells (SW620, SW480, HT29, HCT116, and NCI-H508) were chosen because 5-FU remains the most commonly prescribed agent for advanced stage CRC. We first established the cytotoxic dose of these cell lines (Figure 1C). Interestingly, the IC_{50} for each cell line was highly consistent, exhibiting a range between 3 and 9 μM.

Next, we investigated the global intracellular metabolic changes in CRC cells. The metabolite profile of a panel of CRC cells was assessed 6 hr after treatment with 5-FU, a time point that precedes a majority of the indirect effects of cytotoxicity and cell-cycle processes, while allowing the metabolite effects to be probed. We generated a profile of 339 metabolites and an additional ten compounds that are fluorinated derivatives of 5-FU for the different cells near the IC_{50} dose. An unsupervised hierarchical clustering revealed widespread heterogeneities in metabolite levels across cell lines and in response to 5-FU (Figure S1A; Table S1). Only a few metabolites showed common features across the five CRC cell lines (Figure 2A). However, the major differences in metabolite levels across the panel are observed to be cell-type-specific differences rather than drug-dependent changes, suggesting that metabolism does not exhibit universal global perturbations with this treatment. An examination of the redox and energy status, two measurements of global metabolic changes, shows great variation between the cell lines. Comparing the ratios for 5-FU treated to non-treated cell lines, the NAD^+-mediated redox status is decreased, with increasing NADH/NAD^+ ratios across all cell lines (Figure 2B). In addition, decreasing glutathione (GSH)/glutathione disulfide (GSSG) ratios, indicative of oxidative stress, were observed in all cell lines except the HT29 cell line (Figure 2C). The ATP/ADP ratio also decreased across all the cell lines, implying a decrease in energy metabolism (Figure 2D). To explore this further, we also examined two 5-FU-resistant cell lines, namely MDA-MB-231 and SKOV3, with IC_{50} at 498 and 169 μM, respectively. Both cell lines showed no reduction in either NADH/NAD^+ ratio or ATP/ADP ratio, although they both displayed a decreased ratio of GSH/GSSG (Figure S1C). Taken together, these findings indicate that 5-FU commonly alters global redox and energy metabolism in sensitive cells.

The changes in metabolites upon 5-FU treatment were displayed in a volcano plot for each cell line that showed the fold change and the p value for each metabolite (Figure 2E). The plot indicates order of magnitude changes in certain metabolite concentrations, with up to 30- to 50-fold changes in relative levels being observed. This analysis allowed us to identify commonalities across cells lines (Figures 2F and S1B) that included the accumulation of intracellular 5-FU, an increase in deoxyuridine-monophosphate (dUMP), and surprisingly a depletion of acyl-carnitine compounds. The accumulation of reduced nucleotides, such as deoxyuridine and deoxycytidine-monophosphate (dCMP), was common across cell lines as well. Similarly, intracellular accumulation of 5-FU, deoxyuridine, and dUMP were also found in the two resistant cell lines (Figure S1D). Twenty-four metabolites were affected by 5-FU treatment in two or more CRC cell lines. Pathway analysis of these metabolites revealed that 5-FU showed greatest impact on pyrimidine metabolism, followed by cysteine and methionine metabolism, which is coupled to the folate pool and effects on carnitine metabolism. Also affected were purine and vitamin B6 metabolic pathways (Figure 2G). Given the most commonly altered nucleobase-related metabolites were uridinylated compounds, these findings indicate that thymidylate synthase (TS) is the mechanistic target of 5-FU, likely leading to a direct effect on carnitine metabolism.

Accumulation of Uracil-Related Metabolites at Increasing Doses of 5-FU

Having established the metabolic profile near the IC_{50} dose of 5-FU, we explored the intracellular metabolic profile at different doses of 5-FU. An unsupervised hierarchical clustering revealed that increasing concentrations of 5-FU had an observable effect on a small number of metabolites, either by increasing or decreasing the levels of correlated groups of metabolites (Figure 3A; Table S2). Pathway analysis of metabolites that showed dose-dependent response to 5-FU highlighted in Figure 3A revealed that 5-FU had the most-significant impact on pyrimidine, purine, and vitamin B6 metabolism (Figure 3B). Most metabolites did not exhibit any changes in their levels, and a view of the volcano plot confirmed this observation (Figure 3C). An increasing number of metabolites altered at higher concentrations of 5-FU, with a majority of metabolites remaining fairly constant.

An inspection of the commonalities across doses revealed an accumulation of UXP, dUXP nucleotides, and fluorinated derivatives of nucleic acids at the cytotoxic doses of 5 μM and 100 μM (Figure 3D), confirming again targeted inhibition of TS as a major target of 5-FU. Only at higher doses (100 μM) was the propagation of fluorinated nucleotide metabolism observed beyond a couple steps in the pathway, suggesting that the pro-drug activity of 5-FU that occurs by competing with nucleobases for DNA and RNA metabolism is not occurring at the lethal doses of the compound and not contributing to the cytotoxic mechanism of action. In addition, at nanomolar doses, no metabolites were significantly affected.

A direct comparison of metabolite levels in drug-treated cells to non-treated cells revealed accumulation of uracil and its derivative metabolites at the cytotoxic doses (Figure 3E). dUMP

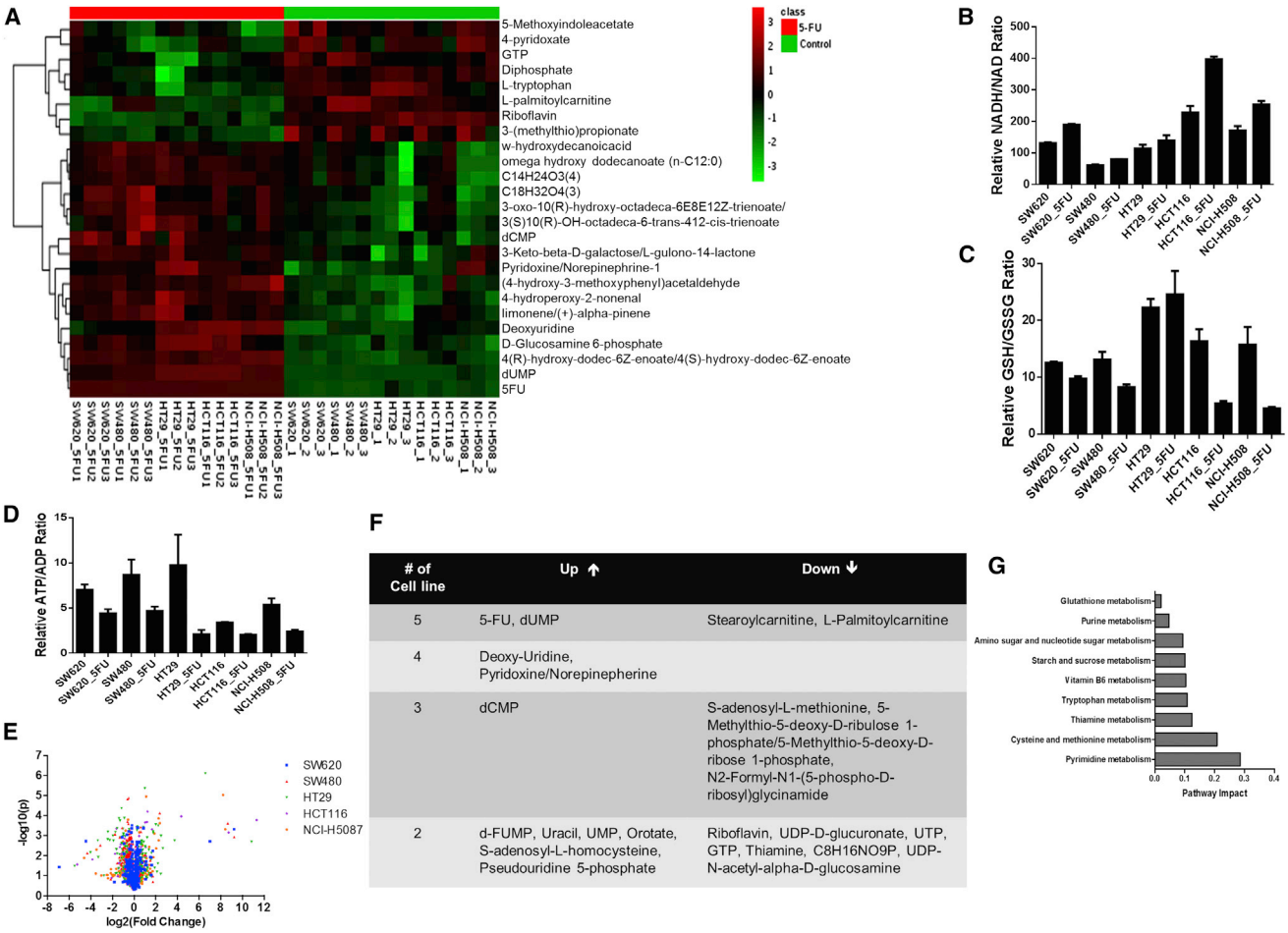

# of Cell line	Up ↑	Down ↓
5	5-FU, dUMP	Stearoylcarnitine, L-Palmitoylcarnitine
4	Deoxy-Uridine, Pyridoxine/Norepinepherine	
3	dCMP	S-adenosyl-L-methionine, 5-Methylthio-5-deoxy-D-ribulose 1-phosphate/5-Methylthio-5-deoxy-D-ribose 1-phosphate, N2-Formyl-N1-(5-phospho-D-ribosyl)glycinamide
2	d-FUMP, Uracil, UMP, Orotate, S-adenosyl-L-homocysteine, Pseudouridine 5-phosphate	Riboflavin, UDP-D-glucuronate, UTP, GTP, Thiamine, C8H16NO9P, UDP-N-acetyl-alpha-D-glucosamine

Figure 2. Commonalities and Heterogeneities in Response to 5-FU

(A) Heatmap of metabolites in five different cancer cell lines. Three hundred fifty-three metabolites were log2, quantile normalized before Pearson hierarchal clustering. Top 25 metabolites exhibiting a common 5-FU pattern were used. See Table S1 for full list of metabolites and Figure S1 for the heatmap of all metabolites.

(B) NADH/NAD ratio.

(C) GSH/GSSG ratio.

(D) ATP/ADP ratio.

(E) Volcano plot for metabolites across the five cell lines.

(F) Metabolites with common changes (fold change > 2 and $p < 0.05$) in two or more cell lines.

(G) Pathway analysis of metabolites in (F).

Error bars represent ± SEM.

and deoxyuridine showed the greatest accumulation with increasing doses of 5-FU. Notably, a slight increase of uridine was observed only at 100 μM 5-FU. A similar pattern was observed for the fluorinated derivatives of nucleic acids (Figure 3F), indicating that metabolite levels are increased only at super-lethal doses of 5-FU and not at lower doses. A closer inspection of metabolite levels reveals that dUMP was increased while deoxy-thymine-triphosphate (dTTP) was decreased at, but not below, the cytotoxic dose of 5-FU (Figure 3G). Levels of deoxyuridine-diphosphate (dUDP) were increased to 4.68-fold by 5 μM 5-FU and 8.95-fold by 100 μM 5-FU. On the contrary, UDP levels were not significantly altered by 5-FU, although an increasing trend was observed at 100 μM dose of 5-FU. These data suggest that TS is inhibited at lethal doses of 5-FU and is likely the initiating event leading to cytotoxicity. Apart from metabolites in the pyrimidine pathway, metabolites involved in one-carbon metabolism were also affected (Figure 3H). Homocysteine levels decreased slightly at higher doses, whereas a general increasing trend was observed for the other metabolites in the pathway as drug dose increases. Notably, in the resistant cell lines treated with 5 μM 5-FU, we saw a commonly reduced dTTP in a less extent in comparison with that in HCT116 cells but no significant accumulation of dUDP or metabolites in one-carbon metabolism (Figure S1D). Together, these findings indicate that specific effects on nucleotide metabolism with concomitant disruptions to other aspects of SGOC metabolism appear to be the mode of action contributing to cytotoxicity by 5-FU.

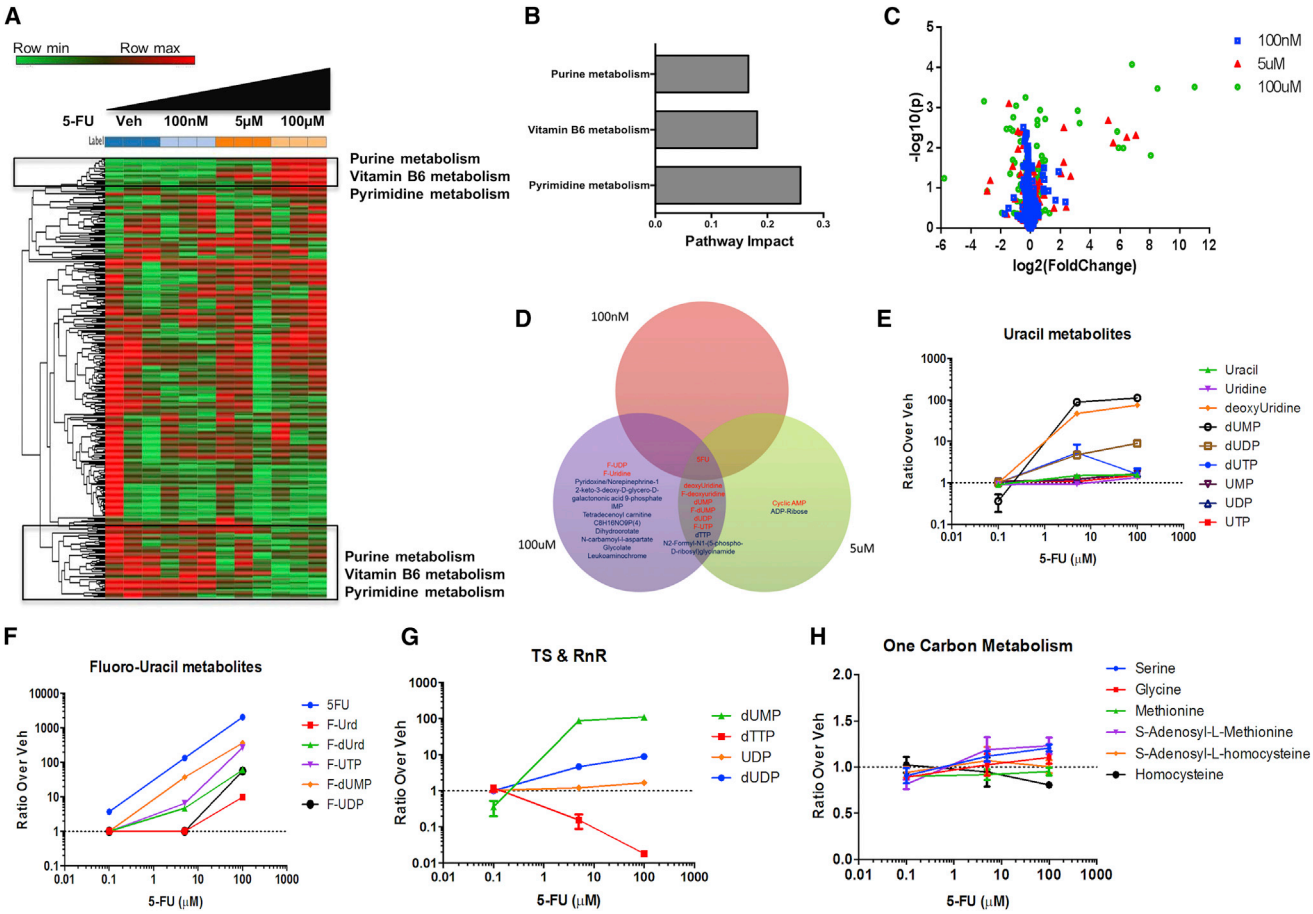

Figure 3. Dose-Dependent Accumulation of Uracil- and 5-Fluorouracil-Derived Metabolites in Intracellular Metabolome

(A) Heatmap for metabolites in HCT116 cells at four doses of 5-FU (0 μM, 100 nM, 5 μM, and 100 μM). See Table S2 for list of metabolites.

(B) Pathway enriched in selected metabolites in (A), with false discovery rate <0.3.

(C) Volcano plot.

(D) Venn diagram of overlapping metabolites altered (fold change > 2 and $p < 0.05$) at different drug doses.

(E–H) Metabolite ratios (5-FU versus vehicle): (E) metabolites derived from uracil; (F) metabolites derived from 5-FU; (G) metabolites involved with TS and RnR; and (H) metabolites in one-carbon metabolism. Error bars represent ± SEM.

Increased Export of Uridine-Related Metabolites Identifies an Overflow Mechanism that Characterizes the 5-FU Response

Thus far, we have profiled metabolites in response to 5-FU treatment in different settings. These findings have indicated that there are specific changes in metabolism related to the point of action in the SGOC network. We next tested whether these changes resulted in the identification of specific metabolic alterations that could have predicative capacity in determining cytotoxicity to 5-FU. Accumulation of uracil and uracil-related metabolites at the cytotoxic doses of 5-FU suggests that the homeostasis of the pyrimidine pathway has been disrupted. Recently, it has been proposed that bacterial cells export excess amounts of uracil-related metabolites and modulate the extent of this export to achieve pyrimidine homeostasis (Reaves et al., 2013). This process is termed overflow metabolism. Given the changes in intercellular metabolism related to pyrimidine biosynthesis, we suspect that these changes might manifest to differences in the secretion rates of nucleotide-related intermediates. To investigate the effects of this disruption on export of metabolites, a flux analysis of secreted compounds was considered.

In response to 5-FU treatment, the levels of excreted uracil from cells remained fairly constant (Figure 4A). 5-FU levels in the media remained fairly constant throughout the treatment as well, indicating that there is no evidence of limitation in 5-FU over the time course (Figure 4B). Pyrimidine-related metabolites accumulated over time, with changes in uridine and deoxyuridine levels at the cytotoxic dose of 5-FU, indicating that export of these metabolites is promoted by 5-FU treatment (Figures 4C and 4D). Apart from metabolites in the pyrimidine pathway, the levels of other metabolites were also altered by 5-FU. Pyruvate and lactate showed decreased levels, when considering higher doses (100 μM) of 5-FU (Figures 4E and 4F). Hypoxanthine showed increased levels when comparing between 5-FU at all doses to the vehicle (Figure 4G). Additionally, methyl-oxopentanoate showed increased levels whereas dihomo-linolenic

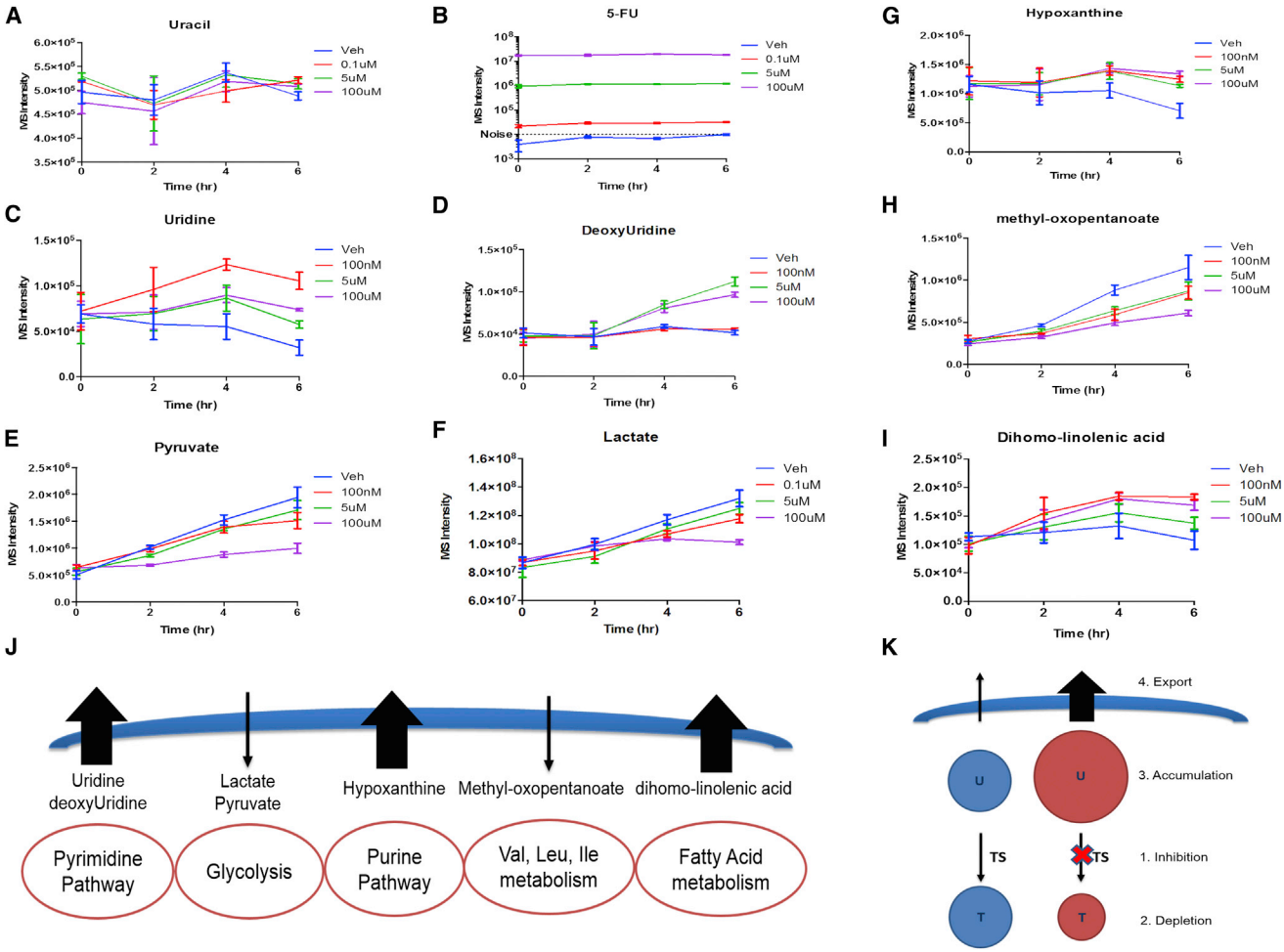

Figure 4. Increase in Uridine and Deoxyuridine Levels in Extracellular Metabolome Suggests Directed Overflow Metabolism

(A–I) Relative quantities of excreted metabolites at 6 hr: (A) uracil; (B) 5-FU; (C) uridine; (D) deoxyuridine; (E) pyruvate; (F) lactate; (G) hypoxanthine; (H) methyl-oxopentanoate; and (I) dihomo-linolenic acid.

(J) Diagram showing metabolites accumulating (arrow up) and decreasing (arrow down) in the extracellular space.

(K) Schematic diagram of overflow metabolism due to 5-FU inhibition.

Error bars represent ± SEM.

acid showed increased levels when comparing between 5-FU at all doses to the vehicle (Figures 4H and 4I). Interestingly, in resistant cell lines, 5-FU (5 μM) caused no overflow of deoxyuridine, and a significantly higher extracellular level of uridine was only found in MDA-MB231 cells (Figure S2). No other common and obvious changes among the other metabolites were observed by 5-FU (Figure S2). Together, these findings point to a model (Figure 4J) whereby a block in TS induces differential export of metabolites proximal in the network to its disruption.

The effect of 5-FU on metabolite excretion, taken together with the intracellular metabolic response, suggests that overflow metabolism is occurring in these mammalian cells and that amount of flux directed into overflow metabolism is affected by the extent of inhibition of TS (Figure 4K). In the presence of 5-FU, TS is inhibited, resulting in depletion of thymine levels and an accumulation of uracil and uracil-derived metabolites. This accumulation of metabolites is then attenuated by increasing export of uridine and deoxyuridine. Hence, overflow metabolism of uridine and deoxyuridine is observed and modulated by the targeting of enzymes involved in pyrimidine metabolism.

Overflow Metabolism Observed in an In Vivo Tumor Response to 5-FU Treatment

The observation of overflow metabolism in the pyrimidine synthesis pathway and that it can be altered by targeting TS with 5-FU lends itself to intriguing possibilities for precision cancer therapy. One possibility would be that, in vivo, the alteration in overflow metabolism would propagate into circulation through the tumor vasculature and result in a directed flow of metabolites in pyrimidine metabolism into the serum. Thus, the relative levels of pyrimidine metabolism intermediates that are present in the serum would determine the extent of 5-FU response. To further investigate the induction of overflow metabolism, non-obese

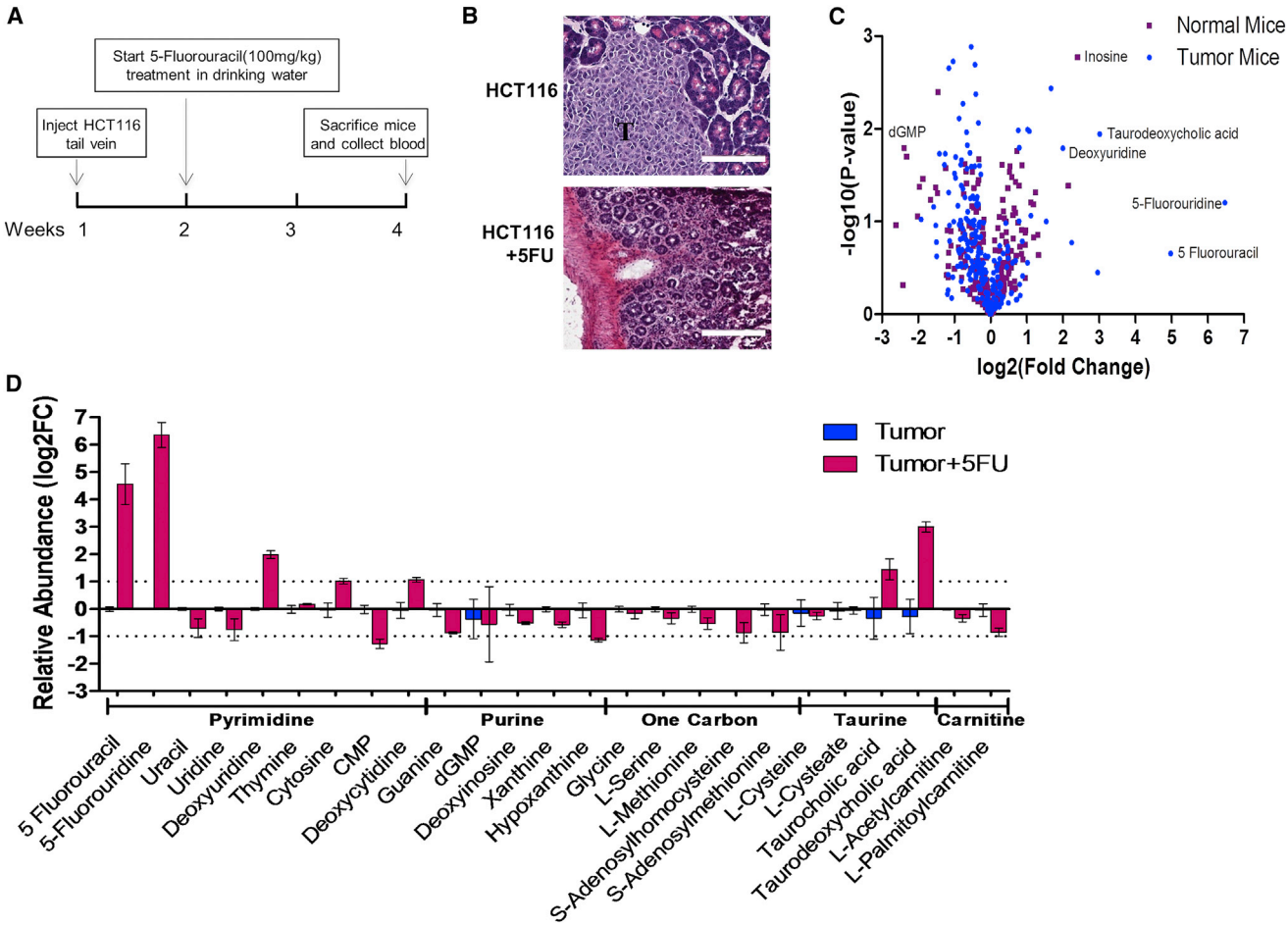

Figure 5. 5-FU Alters Overflow Metabolism In Vivo, and the End Products Can Be Measured in Serum

(A) Experimental design.

(B) H&E staining of colon tissue derived from HCT116-injected tumor-bearing mice treated with or without 5-FU. The scale bar represents 50 μm, which was computed from 40× magnification of histology slide.

(C) Volcano plot of metabolites in normal mice and tumor-bearing mice treated with 5-FU versus mice without treatment.

(D) log2 ratio of metabolite levels in untreated (tumor) and treated (tumor +5-FU) tumor versus normal mouse serum. Error bars represent ± SEM.

diabetic (NOD)/severe combined immunodeficiency (SCID) mice were injected with HCT116 colorectal cancer cells intravenously as previously described and tumors developed orthotopically (Chen et al., 2012). Tumors were allowed to fully develop prior to starting 5-FU treatment (Figure 5A). Tissue sections of mouse colon, stained with H&E, indicate tumor establishment and resolution of colorectal tumors following 5-FU treatment (Figure 5B).

Of the 273 metabolites detected in the serum, most showed minimal changes when comparing the effects of 5-FU treatment to no treatment in both normal and tumor-bearing mice (Figure 5C). Metabolites in tumor-bearing mice showed the largest increases under 5-FU treatment, as compared to normal mice also treated with 5-FU, suggesting that the effects of 5-FU occur primarily in a tumor-autonomous manner. Consistent with directed overflow metabolism, deoxyuridine was found to be greater with log2 (fold change) of 1.998 (p value = 0.016; Student's t test) when comparing 5-FU-treated tumor-bearing mice to untreated tumor-bearing mice. This change was not observed in normal mice when comparing 5-FU treatment to no treatment. Taurodeoxycholic acid, a bile acid generated from the transsulfuration pathway that is related to one carbon metabolism, was also seen in greater quantities when comparing 5-FU-treated to untreated tumor-bearing mice with log2 (fold change) of 3.014 (p value = 0.011; Student's t test). Thus, this suggests that the response to 5-FU has specific effects on the excretion of metabolites from tumors in mice.

Comparing the 5-FU treatment effect in tumor mice to normal mice, 5-FU and 5-fluorouridine levels both increased (Figure 5D). Levels of uracil and uridine in the serum were not significantly altered by 5-FU in tumor-bearing mice, although a trend toward a reduction was observed with log2 (fold change) of −0.614 and −0.637, respectively. Other metabolites that increased significantly are deoxyuridine and taurodeoxycholic acid, indicating that these increases are specific to tumor-bearing mice undergoing 5-FU treatment. In particular, taurodeoxycholic acid is made from taurine, whose precursor is cysteine and

homocysteine. These increases are specific to tumor-bearing mice undergoing 5-FU treatment. All together, these findings provide evidence for directed overflow metabolism and its modulation by an antimetabolite agent in vivo and provide mechanistic insights into potential metabolite biomarkers for monitoring the 5-FU response.

DISCUSSION

These studies allowed us to draw several new conclusions regarding the mechanism of 5-FU action that has been reported to be complex and involve multiple modes of action (Longley et al., 2003; Singh et al., 2015). Our findings appear consistent with the primary mechanism of 5-FU at cytotoxic doses being the disruption of TS activity (Mojardín et al., 2013; Parker and Stivers, 2011). Accumulation of dUMP and decrease of dTTP at the lower dose of 100 nM 5-FU demonstrates inhibition of TS, an enzyme that links the de novo synthesis of thymidine nucleotides to the folate pool (Edler et al., 2002; Etienne et al., 2004; Washtien, 1984). In comparison, the accumulation of fluorinated uridine-triphosphate (UTP) and fluorinated dUMP with subsequent defects in nucleotide biosynthesis and genome maintenance occurred at higher concentrations of 5-FU (100 μM), suggesting that thymidine depletion had a much-greater effect than incorporation of fluorinated nucleotides into DNA. Disruption to the activity of other enzymes involved in the action of 5-FU, including ribonucleotide reductase (RnR) (Elford et al., 1977; Fukushima et al., 2001), was not apparent.

In response to this disruption of TS activity, we found that 5-FU induces a change to an overflow metabolism mechanism previously demonstrated only in bacterial cells (Reaves et al., 2013) but, to our knowledge, has not been shown in mammals. Overflow metabolism, a mechanism to maintain homeostasis in the pyrimidine pathway, results from the accumulation of uracil products caused by limitations to the activity of TS as is observed upon action of 5-FU. In cell culture, accumulation of uracil-derived metabolites and an increase in their extracellular levels upon 5-FU treatment provides direct evidence for this overflow metabolism mechanism. In particular, we observed increased intracellular and extracellular levels of deoxyuridine at higher concentrations of 5-FU (5 μM and 100 μM). Whereas the intracellular level of uridine was only increased at 100 μM of 5-FU, its extracellular level was elevated at all tested concentrations of 5-FU (100 nM, 5 μM, and 100 μM). The lack of corresponding increase of intracellular uridine at 100 nM and 5 μM of 5-FU could be due to increased cellular export of uridine to maintain the cellular homeostasis of uridine. These observations in vitro corroborate with our in vivo study, where 5-FU altered nucleotide flux in tumor-bearing mice, exhibiting changes in deoxyuridine excretion upon 5-FU treatment in serum. It is possible that such a mechanism could potentially be used to stratify patient responses to 5-FU. Supporting this possibility, studies have also shown that uridine supplementation reduces toxicity of 5-FU (van Groeningen et al., 1993), perhaps through reversal of the overflow metabolism.

The metabolite profiling also revealed insights into the effects of 5-FU on other downstream metabolic pathways. In particular, one-carbon metabolism is heavily involved in cancer cell metabolism (Kim et al., 2015; Labuschagne et al., 2014; Maddocks et al., 2013) and might be involved in the cellular response to 5-FU (Locasale, 2013). Correlations with 5-FU cytotoxicity and metabolite export rates show negative correlations of homocysteine and S-adenosyl homocysteine (SAH) levels, whereas our intracellular metabolomics shows decrease in homocysteine levels and an increase in SAH levels. The metabolite levels in tumor-bearing mouse serum show a decrease in detected one-carbon metabolites upon 5-FU treatment. Homocysteine consistently shows up in our analysis and leads to the biosynthesis of taurine and the production of taurodeoxycholic acid. Taurodeoxycholic acid was found in greater quantities in mouse serum when tumor-bearing mouse was treated with 5-FU. This suggests a coupling between folate metabolism and the transsulfuration pathway.

There have been numerous recent findings that have identified molecular mechanisms that underscore the heterogeneity of these pathways in cancer pathogenesis (Locasale, 2013). Although the metabolite profile is diverse across different cell lines, a common response of altering overflow metabolism appears to be a mechanism that is conserved across cells. It is also manifested to in vivo situations in tumor-bearing animals, where it occurred primarily in a tumor-autonomous manner with increased nucleotide secretion. Thus, metabolic profiling the overflow metabolism in patients could possibly yield biomarkers and would provide mechanistic insights into monitoring and stratifying the response of patients to 5-FU. Genetic markers of 5-FU response have been documented (Edler et al., 2002; Etienne et al., 2004), and likely, further analysis will require additional integration of metabolomics with genetics. Nevertheless, our current metabolomics approach emphasizes reliably measurable differences and alterations in the metabolic network. In the future years, simplified cost-effective assays could be developed to specifically quantify smaller panels of metabolites needed to characterize specific metabolic mechanisms. Although this idea is at an early translational stage, our current study provides a mechanistic framework in evaluating therapeutic responses to a conventional, commonly used antimetabolite drug 5-FU, for its more precise use in cancer therapy.

EXPERIMENTAL PROCEDURES

Cell Culture

MDA-MB-231 and SKOV3 cell lines were gifts from Dr. Donald McDonnell and Dr. Alexander Nikitin, respectively. All the other cell lines were gifts from Dr. Lewis Cantley's laboratory. All cells were grown in RPMI 1640 supplemented with 10% fetal bovine serum and 100,000 units/l penicillin and 100 mg/l streptomycin.

Cell Proliferation

Colorectal cancer cell lines (SW620, SW480, HT29, HCT116, and NCI-H508) were seeded in 96-well plates at a density of 2,000–5,000 cells per well. After overnight of incubation, media were replaced with full growth RPMI medium containing 1% DMSO or 5-FU (Sigma) at concentrations (10 nM, 100 nM, 1 μM, 10 μM, 100 μM, and 1 mM) for an additional incubation for 48 hr. Cell viability was determined by crystal violet staining. Further details are provided in the Supplemental Information.

Metabolite Profiling

SW620, SW480, HT29, HCT116, NCI-H508, MDA-MB-231, and SKOV3 cells were seeded in 6-well plates at a density of 2–5 × 10^5 cells per well. After

overnight incubation, cells were washed with PBS and treated with RPMI medium containing vehicle (1% DMSO) or the noted concentration of 5-FU for 6 hr. Metabolite extraction was conducted as previously described (Liu et al., 2014) and detailed in the Supplemental Information.

5-FU Treatment in Colorectal Cancer Xenografts

All animal studies were approved by the Institute for Animal Care and Use Committee at Cornell University. Six- to eight-week-old NOD.Cg-*Prkdc*^{scid} *Il2rg*^{tm1Wjl}/SzJ male mice were used for the study (cat. no. 005557; The Jackson Laboratory). 5×10^5 HCT116 cells were injected in the tail vein. At 2 weeks, 5-FU was introduced into the drinking water of tumor-bearing mice at a dose of 100 mg/kg. At 4 weeks, mice were sacrificed for tissue collection. Tissues were fixed in 4% paraformaldehyde for H&E staining. Serum was snap frozen for metabolomics analysis.

Liquid Chromatography-Mass Spectrometry

Liquid chromatography (Ultimate 3000 Dionex) was coupled to a Q Exactive Mass Spectrometer (Thermo Scientific). Detailed method and analysis are provided in the Supplemental Information.

Statistical Methods

Data represent mean ± SEM unless otherwise noted. All hypothesis testing was conducted with a two-tailed Student's t test unless otherwise noted. * denotes $p < 0.05$ unless otherwise noted.

SUPPLEMENTAL INFORMATION

Supplemental Information includes Supplemental Experimental Procedures, two figures, and two tables and can be found with this article online at http://dx.doi.org/10.1016/j.celrep.2016.05.035.

AUTHOR CONTRIBUTIONS

Z.S., X.G., S.L., and X.L. performed the metabolomics analysis and cell culture experiments. M.M. performed the bioinformatics analysis. C.J. conducted the animal experiments. J.W.L., Z.S., and X.G. designed the study and wrote the manuscript with input from all authors.

ACKNOWLEDGMENTS

Support from NIH R01CA193256 (to J.W.L.) and T32GM007617 (to M.M.), Agency for Science, Technology and Research, Singapore (to Z.S.), and a fellowship from the Duke University School of Medicine (to M.M.) is gratefully acknowledged. We thank Xiling Shen for access to reagents and laboratory space. An invention disclosure related to this study has been filed.

Received: September 17, 2015
Revised: February 11, 2016
Accepted: May 6, 2016
Published: June 2, 2016

REFERENCES

Chen, H.J., Edwards, R., Tucci, S., Bu, P., Milsom, J., Lee, S., Edelmann, W., Gümüs, Z.H., Shen, X., and Lipkin, S. (2012). Chemokine 25-induced signaling suppresses colon cancer invasion and metastasis. J. Clin. Invest. *122*, 3184–3196.

Edler, D., Glimelius, B., Hallström, M., Jakobsen, A., Johnston, P.G., Magnusson, I., Ragnhammar, P., and Blomgren, H. (2002). Thymidylate synthase expression in colorectal cancer: a prognostic and predictive marker of benefit from adjuvant fluorouracil-based chemotherapy. J. Clin. Oncol. *20*, 1721–1728.

Elford, H.L., Bonner, E.L., Kerr, B.H., Hanna, S.D., and Smulson, M. (1977). Effect of methotrexate and 5-fluorodeoxyuridine on ribonucleotide reductase activity in mammalian cells. Cancer Res. *37*, 4389–4394.

Etienne, M.C., Ilc, K., Formento, J.L., Laurent-Puig, P., Formento, P., Cheradame, S., Fischel, J.L., and Milano, G. (2004). Thymidylate synthase and methylenetetrahydrofolate reductase gene polymorphisms: relationships with 5-fluorouracil sensitivity. Br. J. Cancer *90*, 526–534.

Fukushima, M., Fujioka, A., Uchida, J., Nakagawa, F., and Takechi, T. (2001). Thymidylate synthase (TS) and ribonucleotide reductase (RNR) may be involved in acquired resistance to 5-fluorouracil (5-FU) in human cancer xenografts in vivo. Eur. J. Cancer *37*, 1681–1687.

Jain, M., Nilsson, R., Sharma, S., Madhusudhan, N., Kitami, T., Souza, A.L., Kafri, R., Kirschner, M.W., Clish, C.B., and Mootha, V.K. (2012). Metabolite profiling identifies a key role for glycine in rapid cancer cell proliferation. Science *336*, 1040–1044.

Johnson, C.H., Ivanisevic, J., and Siuzdak, G. (2016). Metabolomics: beyond biomarkers and towards mechanisms. Nat. Rev. Mol. Cell Biol.

Kaye, S.B. (1998). New antimetabolites in cancer chemotherapy and their clinical impact. Br. J. Cancer *78* (*Suppl 3*), 1–7.

Kim, D., Fiske, B.P., Birsoy, K., Freinkman, E., Kami, K., Possemato, R.L., Chudnovsky, Y., Pacold, M.E., Chen, W.W., Cantor, J.R., et al. (2015). SHMT2 drives glioma cell survival in ischaemia but imposes a dependence on glycine clearance. Nature *520*, 363–367.

Labuschagne, C.F., van den Broek, N.J., Mackay, G.M., Vousden, K.H., and Maddocks, O.D. (2014). Serine, but not glycine, supports one-carbon metabolism and proliferation of cancer cells. Cell Rep. *7*, 1248–1258.

Liu, X., Ser, Z., and Locasale, J.W. (2014). Development and quantitative evaluation of a high-resolution metabolomics technology. Anal. Chem. *86*, 2175–2184.

Locasale, J.W. (2013). Serine, glycine and one-carbon units: cancer metabolism in full circle. Nat. Rev. Cancer *13*, 572–583.

Locasale, J.W., Grassian, A.R., Melman, T., Lyssiotis, C.A., Mattaini, K.R., Bass, A.J., Heffron, G., Metallo, C.M., Muranen, T., Sharfi, H., et al. (2011). Phosphoglycerate dehydrogenase diverts glycolytic flux and contributes to oncogenesis. Nat. Genet. *43*, 869–874.

Longley, D.B., Harkin, D.P., and Johnston, P.G. (2003). 5-fluorouracil: mechanisms of action and clinical strategies. Nat. Rev. Cancer *3*, 330–338.

Maddocks, O.D., Berkers, C.R., Mason, S.M., Zheng, L., Blyth, K., Gottlieb, E., and Vousden, K.H. (2013). Serine starvation induces stress and p53-dependent metabolic remodelling in cancer cells. Nature *493*, 542–546.

Maddocks, O.D., Labuschagne, C.F., Adams, P.D., and Vousden, K.H. (2016). Serine metabolism supports the methionine cycle and DNA/RNA methylation through de novo ATP synthesis in cancer cells. Mol. Cell *61*, 210–221.

Mehrmohamadi, M., Liu, X., Shestov, A.A., and Locasale, J.W. (2014). Characterization of the usage of the serine metabolic network in human cancer. Cell Rep. *9*, 1507–1519.

Mentch, S.J., Mehrmohamadi, M., Huang, L., Liu, X., Gupta, D., Mattocks, D., Gómez Padilla, P., Ables, G., Bamman, M.M., Thalacker-Mercer, A.E., et al. (2015). Histone methylation dynamics and gene regulation occur through the sensing of one-carbon metabolism. Cell Metab. *22*, 861–873.

Mojardín, L., Botet, J., Quintales, L., Moreno, S., and Salas, M. (2013). New insights into the RNA-based mechanism of action of the anticancer drug 5′-fluorouracil in eukaryotic cells. PLoS ONE *8*, e78172.

Parker, J.B., and Stivers, J.T. (2011). Dynamics of uracil and 5-fluorouracil in DNA. Biochemistry *50*, 612–617.

Possemato, R., Marks, K.M., Shaul, Y.D., Pacold, M.E., Kim, D., Birsoy, K., Sethumadhavan, S., Woo, H.K., Jang, H.G., Jha, A.K., et al. (2011). Functional genomics reveal that the serine synthesis pathway is essential in breast cancer. Nature *476*, 346–350.

Reaves, M.L., Young, B.D., Hosios, A.M., Xu, Y.F., and Rabinowitz, J.D. (2013). Pyrimidine homeostasis is accomplished by directed overflow metabolism. Nature *500*, 237–241.

Ser, Z., Liu, X., Tang, N.N., and Locasale, J.W. (2015). Extraction parameters for metabolomics from cultured cells. Anal. Biochem. *475*, 22–28.

Singh, V., Brecik, M., Mukherjee, R., Evans, J.C., Svetlíková, Z., Blaško, J., Surade, S., Blackburn, J., Warner, D.F., Mikušová, K., and Mizrahi, V. (2015). The complex mechanism of antimycobacterial action of 5-fluorouracil. Chem. Biol. *22*, 63–75.

van Groeningen, C.J., Peters, G.J., and Pinedo, H.M. (1993). Reversal of 5-fluorouracil-induced toxicity by oral administration of uridine. Ann. Oncol. *4*, 317–320.

Washtien, W.L. (1984). Increased levels of thymidylate synthetase in cells exposed to 5-fluorouracil. Mol. Pharmacol. *25*, 171–177.

Ye, J., Fan, J., Venneti, S., Wan, Y.W., Pawel, B.R., Zhang, J., Finley, L.W., Lu, C., Lindsten, T., Cross, J.R., et al. (2014). Serine catabolism regulates mitochondrial redox control during hypoxia. Cancer Discov. *4*, 1406–1417.

Zamboni, N., Saghatelian, A., and Patti, G.J. (2015). Defining the metabolome: size, flux, and regulation. Mol. Cell *58*, 699–706.